Thermodynamic analysis of phase separation in rubber-modified thermosetting polymers: influence of the reactive polymer polydispersity

Carmen C. Riccardi, Julio Borrajo and Roberto J. J. Williams*

Institute of Materials Science and Technology (INTEMA), University of Mar del Plata and National Research Council (CONICET), J. B. Justo 4302, 7600 Mar del Plata, Argentina

(Received 29 December 1993; revised 27 April 1994)

A thermodynamic simulation of the phase separation process in a modified thermosetting polymer was carried out. The polydispersity of the generated polymeric species was taken into account in the frame of a conventional Flory–Huggins equation. The example considered in the simulation was a diglycidyl ether of bisphenol-A (DGEBA)–ethylenediamine (EDA), epoxy–amine polymer, modified by the addition of 15 wt% castor oil (monodisperse modifier). The size increase of the oligomeric species and the corresponding decrease of the entropic contribution to the free energy of mixing made a modifier-rich phase (β-phase) segregate from the matrix (α-phase) at a particular conversion level. The β-phase is enriched in monomers and low-molecular-weight species of the polymer distribution. This produces a significant decrease of the β-phase conversion with respect to the overall conversion. The monomer with the smaller size and functionality is preferentially segregated into the β-phase, leading to a stoichiometric imbalance. When a semipermeable β-phase is assumed, i.e. no oligomeric species are allowed to transfer to the α-phase, a secondary phase separation inside the β-phase is generated. This leads to a sub-matrix (δ-phase) which is rich in modifier, and a sub-segregated phase (γ-phase) which is rich in thermosetting polymer. This process may continue well beyond the gelation of the α-phase, due to the low conversion level of the β-phase at the time the α-phase gels. The thermodynamic simulation explains some recent experimental observations in systems of commercial interest.

(Keywords: rubber-modified thermosets; phase separation; polydispersity)

INTRODUCTION

Low levels of rubbers are often incorporated into normally brittle thermosetting polymers in order to improve the crack resistance and impact strength. This enhancement in toughness results from the separation, during cure, of a randomly dispersed rubbery phase. In this process, the rubber is initially miscible with the resin and curing agent. At a certain conversion, phase separation of the rubber-rich domains starts to take place. As the polymerization proceeds there is an increase in the concentration and size of the dispersed-phase particles[1]. When the matrix gels, this primary separation is practically finished, but a secondary phase separation may continue inside the dispersed-phase particles[2–8].

A phase separation model was developed in order to simulate the morphologies obtained in these systems[3–9]. This model, which is based on a thermodynamic description through a Flory–Huggins equation, and constituent equations for polymerization and phase separation rates, could give a qualitative explanation of the observed experimental trends[3–5,9]. A shortcoming of this description is the use of a pseudo-binary, Flory–Huggins equation to describe the free energy of mixing per unit volume, as follows:

$$\Delta G=(RT/V_1^0)[(\phi_1/Z_1)\ln\phi_1+(\phi_2/Z_2)\ln\phi_2+x\phi_1\phi_2] \quad (1)$$

where the subscript 1 stands for the resin–hardener combination being taken as a pseudo-component (i.e. a diepoxide of functionality 2, cured with a diamine of functionality 4, to generate an epoxy network), the subscript 2 represents the rubber (modifier), R is the molar gas constant, T is the absolute temperature, ϕ is the volume fraction, and x is the interaction parameter. The reference molar volume, V_1^0, is defined on the basis of the number-average molecular weight of the pseudo-component 1; Z_1 and Z_2 are the ratios of the molar volumes of both components, with respect to the component taken as a reference, i.e.

$$Z_1=V_1/V_1^0 \quad (2)$$

$$Z_2=V_2/V_1^0 \quad (3)$$

While Z_2 remains constant during polymerization, Z_1 increases with conversion. For example, for a stoichiometric diepoxide–diamine formulation, the molar volume, based on the number-average molecular weight,

* To whom correspondence should be addressed

0032-3861/94/25/5541-10

increases with the conversion, p, as follows[4,9]:

$$V_1 = V_1^0/(1-4p/3) \quad (4)$$

This equation is valid for $p \leqslant p_{gel}$.

The increase in Z_1 with conversion leads to a significant decrease in the entropic contribution to the free energy of mixing. At a certain conversion, i.e. the cloud-point conversion (p_{cp}), a rubber-rich phase begins to segregate from the matrix.

The utility of equation (1) in predicting the cloud-point conversion of a particular formulation was recently reported[10,11]. Castor oil was used as a monodisperse modifier in a diglycidyl ether of bisphenol-A (DGEBA)–ethylenediamine (EDA) formulation. The interaction parameter, x, was fitted from the cloud-point temperature of the initial (unreacted) system as a function of the amount of castor oil (up to 30 vol%). The cloud-point conversion was predicted from equation (1), by assuming that x was not affected by the polymerization process. The reasonable agreement that was observed between the experimental and predicted values for various temperatures and castor oil concentrations[10,11], proved that phase separation is largely a consequence of the decrease in the entropic contribution (increase in Z_1) to the free energy of mixing during polymerization.

However the pseudo-binary approach cannot be used to explain a number of recent experimental observations:

(1) Both in Lyon (Pascault and coworkers[6–8]), and in Glasgow (Pethrick and coworkers[12]), secondary phase separation occurring inside dispersed domains could be detected for a long period of time after gelation, or even vitrification, of the matrix was observed. The Lyon group[6–8] used a combination of small-angle X-ray scattering (SAXS), light transmission (l.t.), light scattering (l.s.), and transmission (TEM) and scanning (SEM) electron microscopy. The Glasgow group[12] used real-time dielectric measurements.
(2) The asymmetric character of the thermoset α-relaxation peak, as revealed by dynamic mechanical analysis (d.m.a.), was ascribed to a possible stoichiometric imbalance in the thermosetting polymer present in the dispersed-phase particles[13].

In this paper we will give an answer to the following questions. Is there a difference in the extent of reaction (conversion level) between continuous and dispersed phases? How significant is it? Is there a change in the stoichiometry of the thermosetting polymer in both phases?

For this purpose, it is necessary to remove the pseudo-binary approach from the thermodynamic simulation and take into account the distribution of the species generated during polymerization (i.e. the polydispersity of the thermosetting polymer).

The thermodynamic analysis of systems consisting of a polydisperse polymer and a solvent (the modifier in the present case), has been performed by several authors[14–19]. The present analysis will be similar to the one proposed by Kamide *et al.*[17], with the main difference being that the polydispersity of the polymer is not present initially, but is generated during the reaction. Due to the change in the molecular-weight distribution with the conversion of the thermosetting polymer, the thermodynamic analysis has to be carried out for every conversion level. Moreover, the presentation will not be reduced to simple calculations of cloud-point and co-existence curves but situations where only local equilibrium is attained will also be discussed. This represents conditions where diffusion rates are very much slower than polymerization rates, thus leading to a more realistic simulation of the phase separation process in a modified thermosetting polymer.

Such a complex analysis will require us to introduce some hypotheses concerning the dependence of the x parameter. In principle, x must be considered as a function of temperature, composition and number-average degree of polymerization[17], although the effect of molecular weight on the interaction parameter is typically small[14]. Here x will be considered only as a function of the temperature, thus leading to a constant value when studying the phase separation process under isothermal conditions. This proved to be a reasonable assumption for the case of castor-oil-modified epoxies[10,11].

THERMODYNAMIC ANALYSIS

Selected formulation

Although results obtained from the theoretical simulation may be used in a qualitative way to explain/predict the experimental behaviour of a generic rubber-modified thermoset, in order to be able to fix ideas and provide numerical values for the various parameters of the thermodynamic model, a particular formulation will be selected. The system consists of a castor-oil-modified diepoxide (DGEBA)–diamine (EDA) formulation. Relevant parameters for the different chemical species are shown in *Table 1*. This system exhibits the following advantages:

(a) The modifier (castor oil) is a non-reactive monodisperse component, i.e. the only polydispersity effect is the one associated with the oligomeric species generated during the DGEBA–EDA polymerization.
(b) The reaction between the diglycidyl ether of bisphenol-A (DGEBA) and ethylenediamine (EDA) may be regarded as being an ideal polymerization, i.e. the reactivity of the primary and secondary amine hydrogens is almost the same (no substitution effect); intramolecular cyclic species may be neglected[11,20,21].
(c) An experimental study of the phase separation process is available[10,11,22].

A significant characteristic of the selected system is that the hardener (EDA) has a smaller molecular size but a higher functionality than the epoxy resin (DGEBA). As will be discussed later, these characteristics determine the relative segregation of both monomers in the dispersed phase.

Table 1 Relevant parameters of the different chemical species

Species	M (g mol^{-1})	w.p.e.[a] (g)	ρ (g cm^{-3})	f[b]
DGEBA	368	184	1.20	2
EDA	60	15	0.90	4
Castor oil	928	–	0.96	–

[a] Weight per equivalent
[b] Functionality

The simulation will be performed for a stoichiometric DGEBA–EDA system, modified with a volume fraction of castor oil, $\phi_2^0 = 0.177$. This corresponds to a 15 wt% of castor oil in the formulation (a typical value for rubber-modified thermosets). The initial ϕ_2 amount will only be varied when generating the cloud-point curve of the system.

Distribution of species generated during polymerization

The molar concentration of the species generated during polymerization will be denoted as $[E_{m,n}]$, with m and n being, respectively, the number of diamine and diepoxide molecules present in a particular species ($m-1 \leqslant n \leqslant 3m+1$). *Figure 1* shows both of the monomers, $E_{0,1}$ (DGEBA), $E_{1,0}$ (EDA) and one of the possible isomers of $E_{3,5}$. ($E_{m,n}$ includes all of the particular isomers that may be generated with the assumption of no intramolecular reaction.) $E_{m,n}$ has $n-m+1$ unreacted epoxy equivalents and $3m-n+1$ unreacted amine hydrogen equivalents.

The molar concentration of the $E_{m,n}$ species during polymerization was generated from the corresponding kinetic equations (see Appendix). The distribution was truncated for a particular $m_{max} = Z$, such that the weight-average molecular weight of the generated distribution agreed with the theoretical prediction[23] within an error of 0.5%. The details are reported elsewhere[24]. Using Z values of the order of 50, the simulation could be performed up to an epoxy conversion $p_E = 0.50$. (Gelation for the stoichiometric system occurs at $p_E = 0.577$.) Most of the morphological details were generated in this conversion range.

The $E_{m,n}$ species are characterized by the following parameters:

(a) molar mass

$$M_{m,n} = mM_{EDA} + nM_{DGEBA} \tag{5}$$

(b) mass density

$$\rho_{m,n} = M_{m,n} \Big/ \left(m\frac{M_{EDA}}{\rho_{EDA}} + n\frac{M_{DGEBA}}{\rho_{DGEBA}} \right) \tag{6}$$

(c) molar volume

$$V_{m,n} = M_{m,n}/\rho_{m,n} \tag{7}$$

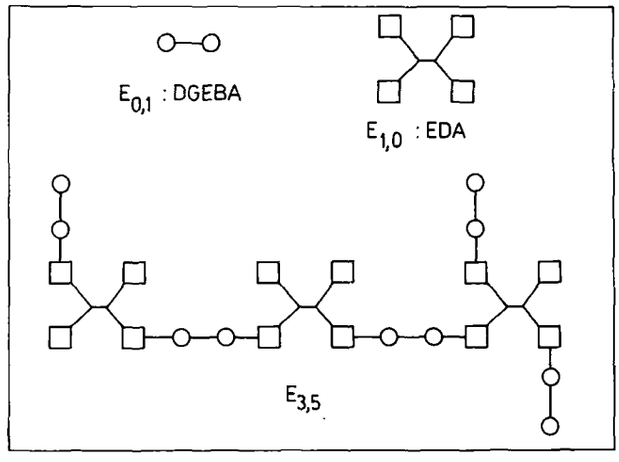

Figure 1 The two monomers and one of the oligomeric species present in the polymer

(d) volume fraction in the solution including modifier

$$\phi_{m,n} = V_{m,n}E_{m,n} \tag{8}$$

The volume fraction of the thermosetting polymer is given by

$$\phi_1 = \sum_m \sum_n \phi_{m,n} \tag{9}$$

while the volume fraction of the modifier is given by:

$$\phi_2 = 1 - \phi_1 \tag{10}$$

Flory–Huggins equation

Equation (1) has to be adapted for the multicomponent system, including every component in the combinatorial term. Now V_1^0 must be replaced by the molar volume of the smallest species, i.e. $V_{1,0} = M_{EDA}/\rho_{EDA}$. The sizes of the various components, measured with respect to the unit cell, are as follows:

$$Z_{m,n} = V_{m,n}/V_{1,0} \tag{11}$$

$$Z_2 = V_2/V_{1,0} \tag{12}$$

where V_2 is the molar volume of castor oil.

The free energy per unit volume is given by the following:

$$\Delta G = (RT/V_{1,0})\left[\sum_m \sum_n (\phi_{m,n}/Z_{m,n}) \ln \phi_{m,n} + (\phi_2/Z_2) \ln \phi_2 + x\phi_1\phi_2 \right] \tag{13}$$

Equation (13) assumes that the interactions between the polymer and the modifier segments may be described by a single parameter (x), independently of the amount of epoxy (n) and amine (m) molecules incorporated in a particular $E_{m,n}$ species. Furthermore, this also means that the interaction of both of the monomers (diepoxide and diamine) with the modifier is considered to be the same. Then, segregation of the $E_{m,n}$ species in the multiphase material will be only determined by their relative sizes (entropic effect). For the particular case of the DGEBA–EDA–castor oil system, the interaction parameter of the DGEBA–castor oil pair is very close to that of a stoichiometric DGEBA–EDA solution, taken as a pseudo-component, with castor oil[10]. For a generic rubber-modified thermosetting polymer, the stoichiometric imbalance generated from phase separation will also depend on the different affinities of the monomers with the modifier.

The interaction parameter for this selected chemical system was previously determined as a function of temperature[10]. A value of $x = 0.28$ was selected, such that the cloud point is attained at a low conversion.

The chemical potentials (μs) may be obtained from equation (13) by the usual procedures[9]:

$$\frac{\Delta\mu_{m,n}}{Z_{m,n}RT} = \frac{1}{Z_{m,n}} + \frac{\ln \phi_{m,n}}{Z_{m,n}} - \left(\frac{\phi_1}{\bar{Z}_{m,n}} + \frac{\phi_2}{Z_2} \right) + x\phi_2^2 \tag{14}$$

$$\frac{\Delta\mu_2}{Z_2RT} = \frac{1}{Z_2} + \frac{\ln \phi_2}{Z_2} - \left(\frac{\phi_1}{\bar{Z}_{m,n}} + \frac{\phi_2}{Z_2} \right) + x\phi_1^2 \tag{15}$$

where $\bar{Z}_{m,n}$ represents the number-average size of the

polymer distribution, measured with respect to the unit cell:

$$\bar{Z}_{m,n}=\frac{\sum_m\sum_n Z_{m,n}E_{m,n}}{\sum_m\sum_n E_{m,n}} \tag{16}$$

In this analysis, the conversion attained in the polymerization is reflected by a particular distribution of the $E_{m,n}$ species arising from the kinetic equations (see Appendix). When the conversion exceeds the cloud point level, two phases will co-exist in equilibrium: a dispersed phase, β, which is rich in modifier and a continuous phase, α, which is rich in polymer. The equilibrium condition requires the following relationships to hold:

$$\Delta\mu^{\alpha}_{m,n}=\Delta\mu^{\beta}_{m,n} \tag{17}$$

$$\Delta\mu^{\alpha}_{2}=\Delta\mu^{\beta}_{2} \tag{18}$$

Combining equations (14) and (15) with equations (17) and (18), respectively, and using $\phi^{\beta}_2=1-\phi^{\beta}_1$ and $\phi^{\alpha}_2=1-\phi^{\alpha}_1$, and then rearranging, we get the following expression for the separation factor, σ_1:

$$\sigma_1=\frac{1}{Z_{m,n}}\ln\left(\frac{\phi^{\beta}_{m,n}}{\phi^{\alpha}_{m,n}}\right)=\frac{\phi^{\beta}_1}{\bar{Z}^{\beta}_{m,n}}-\frac{\phi^{\alpha}_1}{\bar{Z}^{\alpha}_{m,n}}+(\phi^{\alpha}_1-\phi^{\beta}_1)\left[\frac{1}{Z_2}+x(\phi^{\alpha}_1+\phi^{\beta}_1-2)\right] \tag{19}$$

$$\frac{1}{Z_2}\ln\left[\frac{(1-\phi^{\beta}_1)}{(1-\phi^{\alpha}_1)}\right]=\frac{\phi^{\beta}_1}{\bar{Z}^{\beta}_{m,n}}-\frac{\phi^{\alpha}_1}{\bar{Z}^{\alpha}_{m,n}}+(\phi^{\alpha}_1-\phi^{\beta}_1)\left[\frac{1}{Z_2}+x(\phi^{\alpha}_1+\phi^{\beta}_1)\right] \tag{20}$$

The volume fraction of the generic $E_{m,n}$ species, $\phi_{m,n}$, is obtained from solving the kinetic equations up to a certain conversion, in combination with equation (8). The distribution of $\phi_{m,n}$ between the α- and β-phases must satisfy the following balance:

$$\phi_{m,n}=(1-V^{\beta})\phi^{\alpha}_{m,n}+V^{\beta}\phi^{\beta}_{m,n} \tag{21}$$

where V^{β} is the volume fraction of the β-phase ($V^{\alpha}=1-V^{\beta}$).

Substituting σ_1, defined by equation (19), in equation (21), and rearranging, the following is obtained:

$$\phi^{\alpha}_{m,n}=\frac{\phi_{m,n}}{1+V^{\beta}[\exp(\sigma_1 Z_{m,n})-1]} \tag{22}$$

and

$$\phi^{\alpha}_1=\sum_m\sum_n\phi^{\alpha}_{m,n}=\sum_m\sum_n\frac{\phi_{m,n}}{1+V^{\beta}[\exp(\sigma_1 Z_{m,n})-1]} \tag{23}$$

In a similar way, $\phi^{\beta}_{m,n}$ and ϕ^{β}_1 may be obtained, from equations (19) and (21), as follows:

$$\phi^{\beta}_1=\sum_m\sum_n\phi^{\beta}_{m,n}=\sum_m\sum_n\frac{\phi_{m,n}\exp(\sigma_1 Z_{m,n})}{1+V^{\beta}[\exp(\sigma_1 Z_{m,n})-1]} \tag{24}$$

By replacing equations (8) and (11) in equation (16), and then dividing equation (23) by equation (16) (written for α), we get the following:

$$\frac{\phi^{\alpha}_1}{\bar{Z}^{\alpha}_{m,n}}=\sum_m\sum_n\frac{\phi^{\alpha}_{m,n}}{Z_{m,n}}=\sum_m\sum_n\frac{(\phi_{m,n}/Z_{m,n})}{1+V^{\beta}[\exp(\sigma_1 Z_{m,n})-1]} \tag{25}$$

Similarly:

$$\frac{\phi^{\beta}_1}{\bar{Z}^{\beta}_{m,n}}=\sum_m\sum_n\frac{(\phi_{m,n}/Z_{m,n})\exp(\sigma_1 Z_{m,n})}{1+V^{\beta}[\exp(\sigma_1 Z_{m,n})-1]} \tag{26}$$

The set of equations was solved as follows. For a certain conversion, the kinetic equations gave the $\phi_{m,n}$ distribution in the system. Then, by replacing equations (23)–(26) in equations (19) and (20), a system of two equations in two unknowns (σ_1, V^{β}) was obtained, and numerically solved. From equations (21)–(24), $\phi^{\alpha}_{m,n}$, $\phi^{\beta}_{m,n}$, ϕ^{α}_1 and ϕ^{β}_1 (and $\phi^{\alpha}_2=1-\phi^{\alpha}_1$, $\phi^{\beta}_2=1-\phi^{\beta}_1$), were obtained. From knowing the species distribution, the stoichiometric ratios and conversions were calculated separately for each phase. The stoichiometric ratio in a particular phase is defined as follows:

$$r=\text{total amine equivalents/total epoxy equivalents} \tag{27}$$

where 'total' means the sum of the reacted and unreacted equivalents. (The amount of reacted epoxy and amine equivalents is always the same.)

STRATEGIES FOR THE SIMULATION

The simulation was carried out in three different steps, of increasing complexity.

Cloud-point curve

This resulted from the set of equations obtained by making $V^{\beta}\rightarrow 0$. The analysis of the cloud-point and shadow curves provides a first approximation to the qualitative behaviour of the system. The shadow curve gives the compositions of the segregated phase in equilibrium with compositions of the continuous phase located on the cloud-point curve. A comparison of the cloud-point curves obtained for polymerizations carried out with different initial stoichiometries (in one and two steps) has been reported elsewhere[24].

Continuous (α) and dispersed (β) phases at equilibrium

This represents a case where no diffusional limitations are present, i.e. mass transfer proceeds at a much faster rate than polymerization, driving the system towards equilibrium for any conversion. The results obtained will provide a qualitative insight into the evolution of the amount, composition, stoichiometric ratio and conversion of both phases.

Semipermeable β-phase

It is considered that as the β-phase is rich in the viscous modifier, epoxy–amine molecules will remain trapped in the dispersed domains. Therefore, the β-phase will receive material from the continuous phase, but will not deliver molecules back to the α-phase. Consequently, a secondary phase separation will take place inside the β-phase, thus leading to domains rich in epoxy–amine polymer

(γ-phase) which are dispersed in a sub-continuous phase (δ-phase), the latter rich in modifier. This is a situation which resembles more the actual behaviour of a commercial system.

For this case, the thermodynamic simulation was carried out as follows. Once the α- and β-phases had been generated, the kinetic equations were solved independently for both phases. After a 'differential' time, the α-phase was driven to equilibrium, segregating a 'differential' amount of material (rich in modifier) that was incorporated into the β-phase. At this stage the β-phase, modified both by the material received from the α-phase and the evolution of species via continuation of the polymerization, was driven to equilibrium, generating the γ- and δ-phases. This procedure was repeated until the epoxy conversion in the α-phase reached a value close to 0.5. However, as the conversion in the β-phase was very much lower (as will be discussed in the next section), its evolution was followed (now without receiving any material from the α-phase) until the conversion in one of its sub-phases (γ or δ) reached a value close to 0.5.

For every level of conversion, the simulation provided the amount, composition, stoichiometric ratio and conversion of the various phases present in the rubber-modified thermoset.

RESULTS AND DISCUSSION

Cloud-point curve

Figure 2 shows the cloud-point and shadow curves of the system, with epoxy conversion (p_E) vs. modifier volume fraction (ϕ_2) as the coordinates used. Miscibility is affected by the size increase of the polymeric species with conversion. The diagram is valid for a constant temperature, and is related to a selected x value.

For the critical composition, ($\phi_2 \sim 0.35$), the initial formulation ($p_E = 0$) is almost at its cloud point. For $\phi_2^0 = 0.177$ (the typical composition that will be used to simulate the phase separation process), p_E (cloud point) ~ 0.09. This gives us a broad conversion range in which to follow the phase separation process.

Tie lines in *Figure 2* join two phases in equilibrium (one set on the cloud-point curve, with the other on its shadow curve). The shadow curve on the right gives the compositions and conversions of the β-phases segregated from the continuous (α) phase located on the left (i.e. at low values of ϕ_2). Two facts are obvious: first, the segregated phase has a large amount of epoxy–amine polymer dissolved in the modifier; secondly, the conversion in the dispersed phase is lower than that in the continuous phase. This is a consequence of the polymer fractionation: monomers and low-molecular-weight species are segregated into the dispersed phase. As previously discussed, this fractionation arises exclusively from the difference in sizes (and not in the relative amount of epoxy and amine blocks present in the oligomeric species).

Figure 3 shows the stoichiometric ratio of the epoxy–amine polymer segregated from the matrix at the cloud point, as a function of the modifier volume fraction. The continuous phase remains stoichiometric ($r = 1$ for the cloud-point curve), because only a differential volume fraction of the dispersed phase is generated. However, a significant departure from stoichiometry may occur in the segregated phase, depending on the initial volume fraction of the modifier. To explain the observed trend

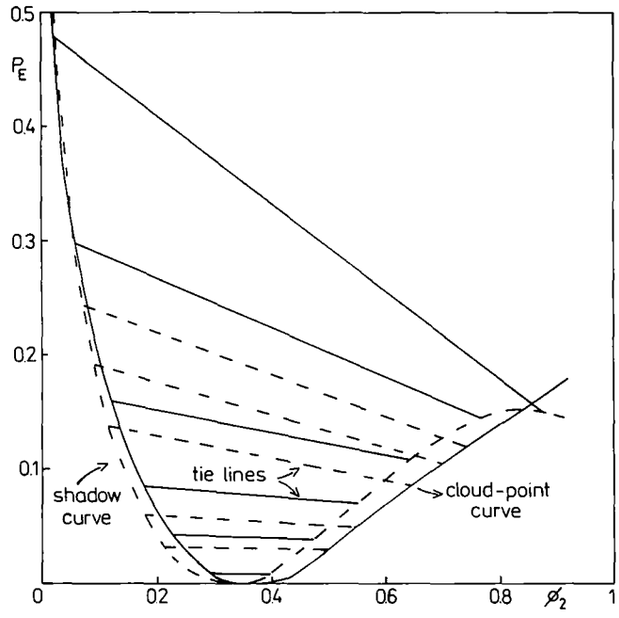

Figure 2 Cloud-point and shadow curves of the system, using epoxy conversion vs. modifier volume fraction as coordinates

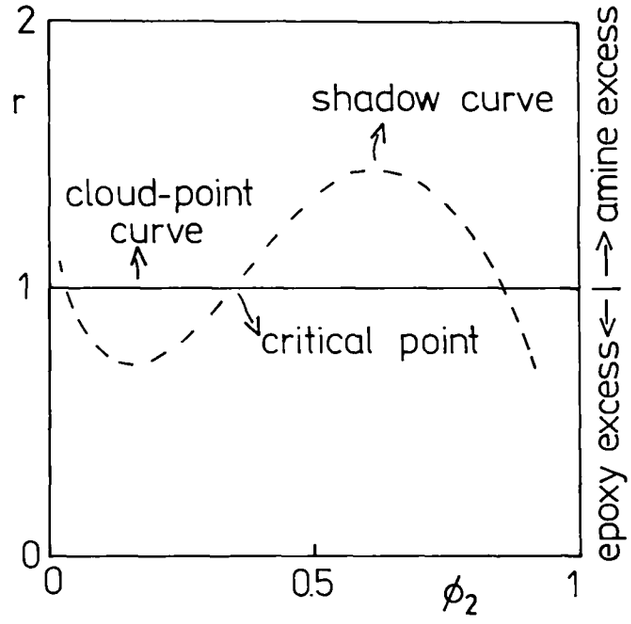

Figure 3 Ratio of the amine/epoxy equivalents segregated from the matrix at the cloud point vs. modifier volume fraction, for an initial stoichiometric formulation ($r = 1$)

let us start at the composition of the critical point ($\phi_{2,crit}$) and observe the variation in stoichiometry of the shadow curve composition when moving towards the right. This means that we are *decreasing* the initial volume fraction of modifier in the formulation. (From *Figure 2*, this means an increase in both the cloud-point conversion and the ϕ_2 value of the shadow curve.) Due to the smaller size of the diamine monomer with respect to the diepoxide monomer, the segregated phase shows an increase in the amine/epoxy ratio. (The modifier is always more compatible with the smallest-size species of the polymer distribution.) However, at a certain point the trend is

reversed. For example, for a segregated phase with $\phi_2 = 0.875$, the initial ϕ_2^0 in the continuous phase is close to 0.02, as revealed from the tie line plotted in *Figure 2*. The cloud-point conversion corresponding to this composition is $p_E = 0.48$. For an ideal polymerization, the fraction of monomer with the functionality f, remaining at a conversion p, is given by:

$$\text{fraction of unreacted monomer} = (1-p)^f$$

Therefore, at $p_E = 0.48$, the fraction of free diamine monomer ($f=4$) is 0.073, whereas the fraction of the free diepoxide monomer ($f=2$) is 0.270. As there is much more epoxy than amine monomer, the segregated phase becomes richer in epoxy at high cloud-point conversions.

A similar explanation may be given for the variations of the shadow curve stoichiometry for $\phi_2 < \phi_{2,crit}$ (*Figure 3*). Therefore, for the range of initial concentrations $\phi_2^0 < \phi_{2,crit}$ (the range of practical interest), the segregated phase is a solution containing a large amount of epoxy–amine species. The polymer distribution is rich in low-molecular-weight species, and particularly in both monomers. Then, the conversion of the segregated phase is always less than that of the continuous phase. The conditions for one of the monomers to prevail over the other in the dispersed phase are as follows: a smaller size (favours the solubility in the modifier through a higher entropic contribution) and a higher concentration in the continuous phase for a given conversion. (The monomer with the lower functionality is favoured, particularly at high conversions.) If, as in the case under analysis here, the smallest monomer has the highest functionality, then the stoichiometric ratio in the dispersed phase will depend on the cloud-point conversion. (At low conversions the size effect prevails over the influence of functionality.)

Continuous (α) *and dispersed* (β) *phases at equilibrium*

In this case, it is assumed that both phases attain equilibrium for every conversion level. *Figure 4* shows the evolution of the primary morphology, i.e. the dispersed domains (β-phase) segregated from the matrix (α-phase), for an initial volume fraction of modifier, $\phi_2^0 = 0.177$. It is again observed that the conversion in the segregated phase is significantly lower than the overall conversion, p_E^0. This is due to the preferential segregation of monomers and low-molecular-weight species into the β-phase.

The evolution of several parameters characterizing the phase separation process is depicted in *Figure 5* as a function of the overall epoxy conversion in the system, p_E^0. *Figure 5a* shows a fast increase in V^β in the conversion range near the cloud point, followed by the attainment of an almost constant value at high conversions. This arises from the shape of the coexistence curve shown in *Figure 4*; therefore most of the primary morphology is determined at conversions close to the cloud point[11]. How would this curve be modified in the presence of diffusional limitations? As the diffusion coefficient is inversely proportional to the viscosity through the Stokes–Einstein equation[3], and as the viscosity increases significantly with conversion, it is expected that mass transfer limitations will limit the increase in V^β, particularly at high conversions. Therefore, a sharp increase of V^β to its final value, over a narrow conversion

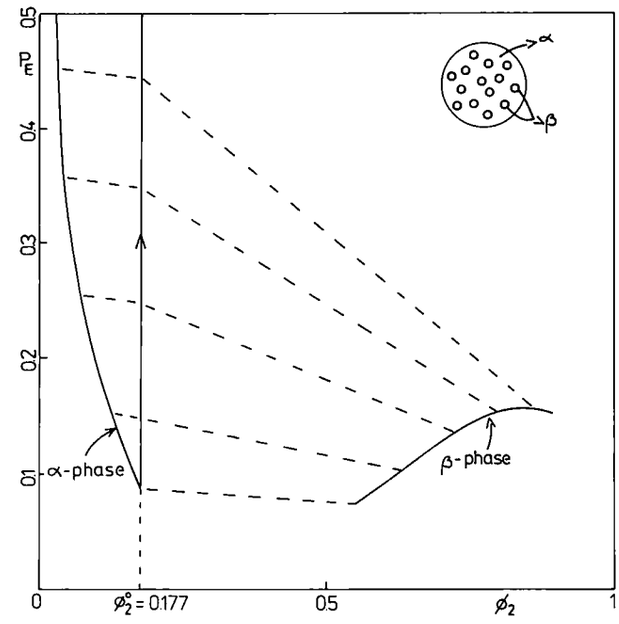

Figure 4 Conversion and composition of the phases at equilibrium (coexistence curves) for an initial volume fraction of modifier, $\phi_2^0 = 0.177$

range close to the cloud-point conversion, is expected in the presence of diffusional limitations.

Figure 5b shows the evolution of the modifier volume fraction in both phases. It is observed that, even in this limiting case where the system is driven to equilibrium, at conversions close to gelation the α-phase still contains some dissolved rubber, while the β-phase includes a significant concentration of epoxy–amine polymer. (No primary phase separation is experimentally observed beyond gelation.)

Figure 5c shows the variation in the ratios of the amine/epoxy equivalents in both phases. The β-phase is initially enriched in the amine, but at higher conversions the epoxy groups prevail over the amine hydrogens. The reasons for this have been discussed in the previous section. Naturally, the α-phase shows the opposite behaviour. However, as the volume fraction of the β-phase, V^β, is rather low, only small departures of the α-phase composition from stoichiometry are observed.

The conversions of the epoxy–amine polymer (in both phases) are plotted in *Figure 5d*. Conversions in the β-phase are very much lower than conversions in the α-phase. Of interest is the fact that while initially the epoxy conversion (p_E^β) is higher than the amine conversion (p_A^β), at high values of p_E^0 the trend is reversed. Moreover, p_E^β begins to *decrease* when increasing p_E^0. This is again due to the fact that at high values of p_E^0, the β-phase becomes rich in the monomer with the lower functionality (the epoxy monomer). Then, the relative fraction of the unreacted epoxy groups in the β-phase shows an increase with p_E^0, i.e. p_E^β decreases at high values of p_E^0.

Semipermeable β*-phase: generation of a secondary structure*

In this case, the segregated β-phase is semipermeable, i.e. it receives, but does not deliver material back to the continuous α-phase. (Epoxy–amine molecules are

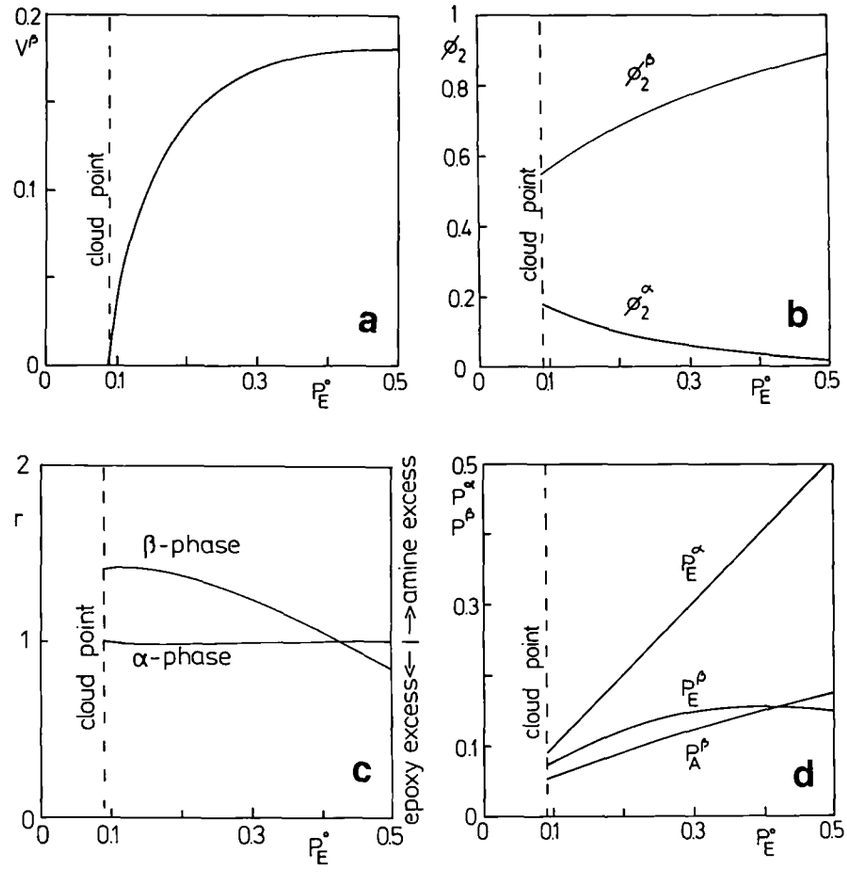

Figure 5 Phase separation parameters as a function of the overall epoxy conversion in the system, p_E^0: (a) volume fraction of the dispersed phase; (b) volume fractions of the modifier; (c) ratios of amine/epoxy equivalents; (d) epoxy and amine conversions

trapped in the β-phase due to the high viscosity of a solution rich in modifier.) This leads to a secondary phase separation inside the β-phase, i.e. a dispersed γ-phase, rich in epoxy–amine polymer, and a continuous δ-phase, rich in modifier (trapping the γ domains in its interior). This situation is depicted in *Figure 6*, starting with an initial volume fraction of modifier, $\phi_2^0 = 0.177$. While the γ–β–δ tie lines join phases at equilibrium, the α–β lines represent two phases that co-exist at a certain polymerization time. Several characteristics of the phase separation process are described in *Figure 7*, as a function of the epoxy conversion in the α-phase.

Figure 7a shows the variations in the volume fractions of the dispersed phase, V^β, and of the sub-phases present in the secondary structure, i.e. V^γ and V^δ. It is observed that although V^β increases at a faster rate at conversions close to the cloud point, it does not reach an almost asymptotic value as in the previous case. This is the result of the semipermeable character of the β-phase, i.e. it receives material from the α-phase, but does not deliver any material back. In an actual system, diffusional limitations will again ensure that most of the primary phase separation (i.e. generation of the β-phase), takes place in a narrow conversion range close to the cloud point.

A sub-structure is generated inside the β-phase, starting at conversions close to the cloud point. This agrees with the experimental results obtained by Chen *et al.*[7,8], using

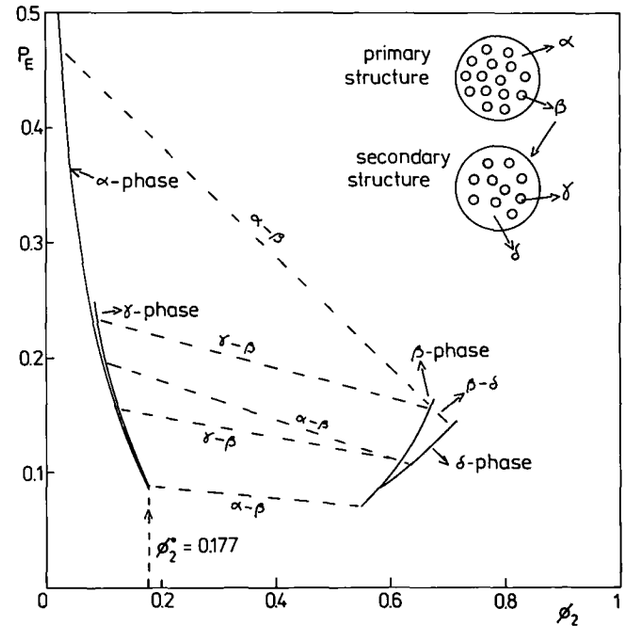

Figure 6 Conversion and composition of phases co-existing during the polymerization process when the β-phase is semipermeable (initial volume fraction of modifier, $\phi_2^0 = 0.177$)

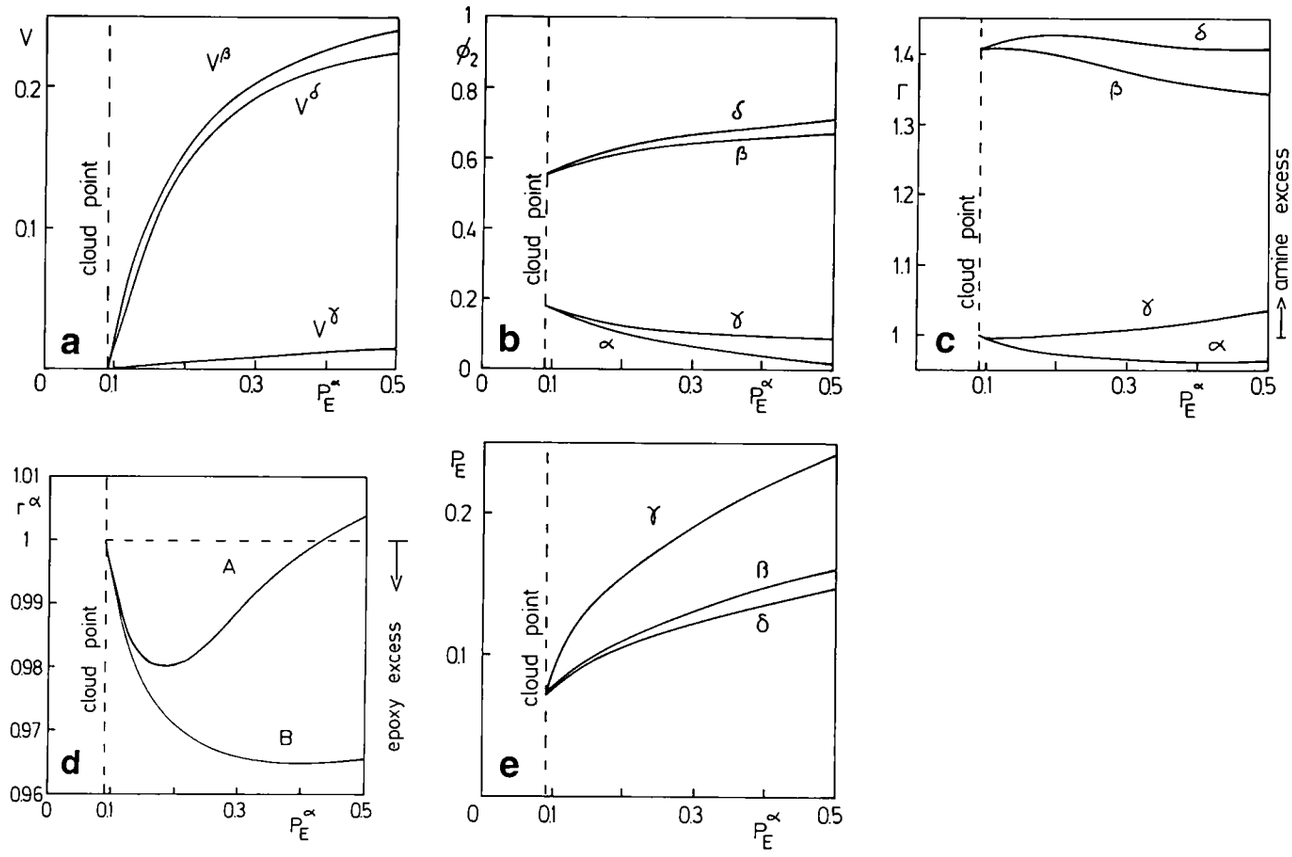

Figure 7 Phase separation parameters as a function of the epoxy conversion in the α-phase (a) volume fractions of the different phases; (b) volume fractions of the modifier; (c) ratios of amine/epoxy equivalents; (d) comparison of the ratios of the amine/epoxy equivalents in the α-phase for the permeable β-phase (A), and the semipermeable β-phase (B); (e) the epoxy conversions in the dispersed domains

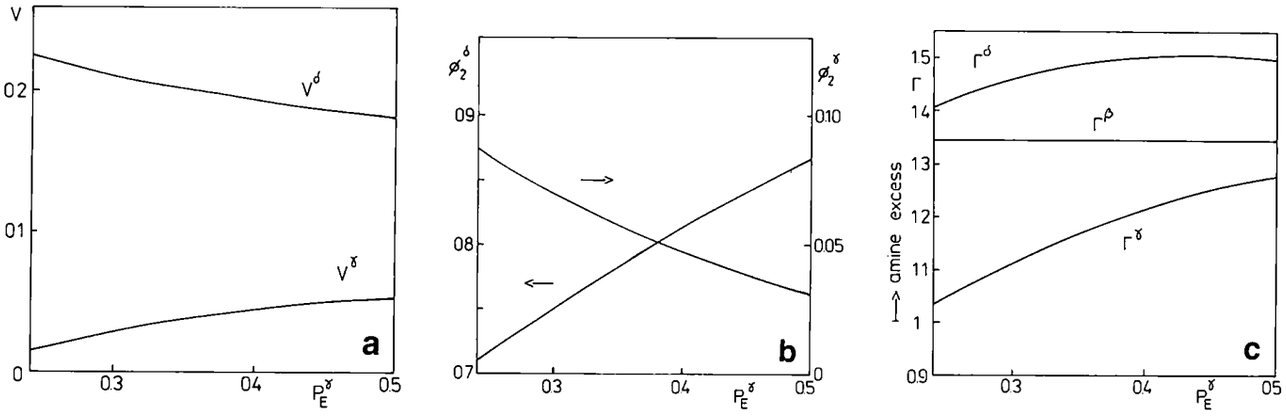

Figure 8 Evolution of phase separation parameters in the secondary structure, as a function of the epoxy conversion in the γ-phase, after the β-phase becomes impermeable to mass transfer: (a) volume fractions of the δ- and γ-phases; (b) volume fractions of the modifier; (c) ratios of amine/epoxy equivalents

a SAXS technique. A significant fact is that as conversions in both the γ- and δ-phases are low (*Figure 6*) there is no reason why secondary phase separation should stop when the α-phase gels (or even vitrifies). Then, V^{γ} may continue to increase at the expense of V^{δ}, as will be discussed later. This gives an explanation to some recent experimental observations[6-8,12], where the secondary phase separation was observed well beyond gelation or vitrification of the matrix (α-phase).

Figure 7b shows the evolution of the modifier volume fraction in the different phases. Due to the semipermeable character of phase β and the fact that most of the primary phase separation takes place at conversions close to the cloud point, ϕ_2^{β} reaches a maximum value close to 0.67, i.e. much lower than in the previous case. This means that in an actual system a significant fraction of thermosetting polymer will remain trapped in the dispersed phase domains.

Evolution of the ratios of the amine/epoxy equivalents in the different phases is shown in *Figure 7c*. Now, due to its semipermeable character, the β-phase retains the excess diamine monomer segregated at low conversions.

This leads to a significant departure from stoichiometry in the dispersed phase domains. The matrix (α-phase) is deficient in amine, but the departure from stoichiometry is not so significant. *Figure 7d* shows the evolution of the stoichiometric ratio in the matrix (using an amplified scale). A comparison between the previous case (A, α- and β-phases in equilibrium) and the present case (B, semipermeable β-phase), is provided. It is observed that in the present case the initial amine segregation is not recovered, thus leading to a final matrix with the r value close to 0.965.

Figure 7e shows the evolution of the epoxy conversion in the dispersed domains. When the matrix is approaching gelation, the overall epoxy conversion in the dispersed domains is $p_E^\beta < 0.2$. This means that secondary phase separation should be observed, when using the appropriate techniques[6-8,12], for a long period of time after matrix gelation. Now, as the modifier is always more miscible with the low-molecular-weight species, the segregated γ-phase in the secondary structure is therefore more converted than the sub-continuous δ-phase, which is rich in modifier (*Figure 7e*).

In order to follow the evolution of the secondary structure after gelation of the matrix, it was assumed that mass transfer from the α- to the β-phases was arrested at $p_E^\alpha = 0.5$, i.e. after this (conversion) β-phase remained impermeable to further mass transfer. The increase in the β-phase conversion leads to a continuous increase in the volume fraction of the γ-phase (at the expense of the δ-phase), as shown in *Figure 8a*. The simulation was stopped at $p_E^\gamma = 0.5$, but the actual process could be further continued as the conversion in the δ-phase, $p_E^\delta = 0.24$ when $p_E^\gamma = 0.5$.

Figure 8b shows the evolution of the composition of the γ- and δ-phases. The trend is to increase the purity of both sub-phases, i.e. a γ-phase very rich in epoxy–amine polymer (although some amount of modifier will be retained after gelation), and a δ-phase that may be regarded as consisting of almost pure modifier after phase separation is complete, i.e. a very diluted solution of diamine and diamine-end-capped diepoxides in the modifier. This excess amine is also present in the γ-phase, as revealed in *Figure 8c*.

CONCLUSIONS

A thermodynamic simulation of the phase separation process in modified thermosetting polymers was performed, taking into account the polydispersity of the polymeric species that were generated.

The size increase of the oligomeric species and the corresponding decrease in the entropic contribution to the free energy of mixing, caused a modifier-rich phase (β-phase) to segregate from the matrix (α-phase) at a particular conversion level. The β-phase contains a significant amount of low-molecular-weight species of the polymer distribution. In particular, both monomers are selectively segregated into the dispersed phase. This produces a significant decrease in the dispersed phase conversion with respect to the overall conversion. The relative concentration of both monomers in the β-phase may differ from that in the initial formulation. This leads to a departure from stoichiometry for both phases, a fact that is enhanced in the dispersed phase due to its smaller volume fraction. When there is not a preferential interaction energy between the modifier and one of the monomers (an hypothesis of the performed simulation), the monomer whose relative concentration is increased in the β-phase is the one with the smaller values of size and functionality (i.e. the number of reactive groups per molecule). If the monomer with the smaller size has a higher functionality (e.g. the diamine used in this present simulation), it will be preferentially segregated into the β-phase at low conversions, but this trend will be reversed at high conversions.

Due to the high viscosity of commercial modifiers, there is a diffusional resistance in the case of the epoxy–amine polymer segregated into the β-phase, to be partially recovered by the α-phase, as required by the thermodynamic equilibrium when conversion increases. This situation was simulated by assuming that the β-phase was semipermeable to mass transfer. Under these conditions, a secondary phase separation takes place inside the dispersed domains. This leads to a sub-matrix (δ-phase) which is rich in modifier, and a sub-segregated phase which is rich in thermosetting polymer (γ-phase). This process may continue well beyond gelation of the α-phase due to the low conversion level of the β-phase at the time the α-phase gels. The composition of the γ- and δ-phases may become very close to that of the pure epoxy–amine polymer and modifier, respectively. However a significant stoichiometric imbalance may be observed in the epoxy–amine polymer present in both phases.

Aspects of the predicted behaviour (i.e. secondary phase structure generated well after matrix gelation[6-8,12]) have been experimentally observed; other trends, such as the presence of a significant stoichiometric imbalance in the dispersed domains, are yet to be investigated. In any case, the thermodynamic simulation provides a theoretical framework for explaining the phase separation process in rubber-modified thermosets.

REFERENCES

1 Visconti, S. and Marchessault, R. H. *Macromolecules* 1974, **7**, 913
2 Manzione, L. T., Gillham, J. K. and McPherson, C. A. *J. Appl. Polym. Sci.* 1981, **26**, 889, 907
3 Williams, R. J. J., Borrajo, J., Adabbo, H. E. and Rojas, A. J. in 'Rubber-Modified Thermoset Resins' (Eds C. K. Riew and J. K. Gillham), ACS Advances in Chemistry Series, Vol. 208, American Chemical Society, Washington, DC, 1984, p. 195
4 Moschiar, S. M., Riccardi, C. C., Williams, R. J. J., Verchère, D., Sautereau, H. and Pascault, J. P. *J. Appl. Polym. Sci.* 1991, **42**, 717
5 Verchère, D., Sautereau, H., Pascault, J. P., Moschiar, S. M., Riccardi, C. C. and Williams, R. J. J. in 'Toughened Plastics I: Science and Engineering' (Eds C. K. Riew and A. J. Kinloch), ACS Advances in Chemistry Series, Vol. 233, American Chemical Society, Washington, DC, 1993, p. 335
6 Grillet, A. C., Galy, J. and Pascault, J. P. *Polymer* 1992, **33**, 34
7 Chen, D. *PhD Thesis*, INSA de Lyon, France, 1992
8 Chen, D., Pascault, J. P., Sautereau, H. and Vigier, G. *Polym. Int.* in press
9 Vázquez, A., Rojas, A. J., Adabbo, H. E., Borrajo, J. and Williams, R. J. J. *Polymer* 1987, **28**, 1156
10 Ruseckaite, R. A. and Williams, R. J. J. *Polym. Int.* 1993, **30**, 11
11 Ruseckaite, R. A., Hu, L., Riccardi, C. C. and Williams, R. J. J. *Polym. Int.* 1993, **30**, 287
12 Delides, C. G., Hayward, D., Pethrick, R. A. and Vatalis, A. S. *J. Appl. Polym. Sci.* 1993, **47**, 2037
13 Verchère, D., Pascault, J. P., Sautereau, H., Moschiar, S. M., Riccardi, C. C. and Williams, R. J. J. *J. Appl. Polym. Sci.* 1991, **42**, 701

14 Koningsveld, R. and Staverman, A. J. *J. Polym. Sci. (A-2)* 1968, **6**, 305, 325
15 Solc, K. *Macromolecules* 1970, **3**, 665
16 Kamide, K. and Miyazaki, Y. *Polym. J.* 1981, **13**, 325
17 Kamide, K., Matsuda, S. and Shirataki, H. *Eur. Polym. J.* 1990, **26**, 379
18 Rätzsch, M. T. *Makromol. Chem., Macromol. Symp.* 1987, **12**, 101
19 Mumby, S. J., Sher, P. and Eichinger, B. E. *Polymer* 1993, **34**, 2540
20 Riccardi, C. C., Adabbo, H. E. and Williams, R. J. J. *J. Appl. Polym. Sci.* 1984, **29**, 2481
21 Riccardi, C. C. and Williams, R. J. J. in 'Crosslinked Epoxies' (Eds B. Sedlácek and J. Kahovec), de Gruyter, Berlin, 1987, p. 291
22 Ruseckaite, R. A., Fasce, D. P. and Williams, R. J. J. *Polym. Int.* 1993, **30**, 297
23 Stockmayer, W. H. *J. Polym. Sci.* 1952, **9**, 69
24 Riccardi, C. C. and Borrajo, J. *Polym. Int.* 1993, **32**, 241
25 Bajpai, A. C., Mustoe, L. R. and Walker, P. 'Advanced Engineering Mathematics', John Wiley and Sons, Chichester, 1977, p. 134

APPENDIX

Generation of the distribution of chemical species

Kinetic equations are written in terms of dimensionless concentrations $[E_{m,n}] = E_{m,n}/(E_{0,1})_0$ and a dimensionless time, $\tau = k(E_{0,1})_0^2 t$, where k is the specific rate constant of the epoxy–amine reaction catalysed by OH groups[11]. The concentration of OH groups increases during polymerization, with one of these groups being the result of the reaction between an epoxy group and an amine hydrogen.

The following set of kinetic equations may be written:

$$\frac{d[E_{0,1}]}{d\tau} = -2[OH][E_{0,1}] \sum_{m=1}^{z} \sum_{n=m-1}^{3m+1} (3m-n+1)[E_{m,n}] \tag{A1}$$

$$\frac{d[E_{1,0}]}{d\tau} = -4[OH][E_{1,0}]\left[2[E_{0,1}] + \sum_{n=1}^{4} n[E_{1,n}] + \sum_{m=2}^{z} \sum_{n=m-1}^{3m+1} (n-m+1)[E_{m,n}]\right] \tag{A2}$$

$$\left.\frac{d[E_{1,n}]}{d\tau}\right|_{1 \leqslant n \leqslant 4} = 2(5-n)[OH][E_{0,1}][E_{1,n-1}] - [OH][E_{1,n}]\left[n\left(\sum_{a=1}^{z-m} \sum_{b=a-1}^{3a+1} (3a-b+1)[E_{a,b}]\right) + (4-n)\left(\sum_{a=1}^{z-m} \sum_{b=a-1}^{3a+1} (b-a+1)[E_{a,b}] + 2[E_{0,1}]\right)\right] \tag{A3}$$

$$\left.\frac{d[E_{m,n}]}{d\tau}\right|_{\substack{m>1 \\ m-1 \leqslant n \leqslant 3m+1}} = 2(3m-n+2)[OH][E_{0,1}][E_{m,n-1}] + \sum_{a=1}^{m-1} \sum_{b=b_{min}}^{b_{max}} [E_{a,b}][E_{m-a,n-b}][OH] (3a-b+1)(n-b-m+a+1) - [OH][E_{m,n}]\left[(n-m+1)\left(\sum_{a=1}^{z-m} \sum_{b=a-1}^{3a+1} (3a-b+1)[E_{a,b}]\right) + (3m-n+1)\left(\sum_{a=1}^{z-m} \sum_{b=a-1}^{3a+1} (b-a+1)[E_{a,b}] + 2[E_{0,1}]\right)\right] \tag{A4}$$

where

$$b_{max} = \begin{cases} n-m+a+1 & \text{if } n < (2a+m) \\ 3a+1 & \text{if } n \geqslant (2a+m) \end{cases}$$

$$b_{min} = \begin{cases} a-1 & \text{if } n < (3m-2a) \\ 3a-3m+n-1 & \text{if } n \geqslant (3m-2a) \end{cases}$$

Equations (A1) to (A4) were solved by using a fourth-order Runge–Kutta method[25].